

# Identification and Handling of Critical Constraints in Time-Constrained SCOPF Analysis of Power Systems

J. Gunda, D. Fang and S. Djokic

School of Engineering  
The University of Edinburgh  
Edinburgh, Scotland, UK  
[Sasa.Djokic@ed.ac.uk](mailto:Sasa.Djokic@ed.ac.uk)

M. Lehtonen

Department of Electrical Engineering  
Aalto University  
Aalto, Finland  
[Matti.Lehtonen@aalto.fi](mailto:Matti.Lehtonen@aalto.fi)

**Abstract**—Provision of accurate, flexible, computationally efficient and robust analytical and modelling tools is essential for ensuring optimal design and secure operation of power supply systems. This paper demonstrates how conventional gradient-based security constrained optimal power flow (SCOPF) methods can be improved for the analysis of power supply networks with severe multiple contingencies. In such cases, conventional SCOPF methods may fail to converge and paper demonstrates how metaheuristic methods with a suitable penalty constraint handling can identify the “critical constraints” and provide solution in which all other (except these critical) constraints will be satisfied by adjusting primary controls. Further evaluation of critical constraints in terms of available response time for activation of secondary controls allows to introduce “time-constrained SCOPF analysis”, which is then used to devise corrective actions for returning the system into a feasible operating region. A novel formulation of “dynamic penalty function”, based on dynamic thermal rating of overloaded lines, and evaluation of the most effective corrective action, e.g. “selective load shedding”, are illustrated on a commonly used IEEE 14-bus test network.

**Keywords**—Conventional and metaheuristic optimization; security constrained optimal power flow; time-constrained analysis.

## I. INTRODUCTION

Optimal power flow (OPF) analysis is a well-established and important tool for evaluating performance of electricity networks at both planning and operational stages. Depending on the target applications, OPF studies can include a wide range of objective functions, various controls and diverse operational/security requirements as constraints [1]. Traditional OPF studies are aimed at the analysis of normal operating conditions, while security-constrained OPF (SCOPF) studies consider steady state network security constraints, e.g. bus voltages and line loading limits, for both normal operating conditions and for a set of known, credible or expected contingencies [2]. In that context, SCOPF studies are used to plan or devise preventive and/or corrective control actions that will return the system into a normal or feasible operating region following a contingency, e.g. a system fault.

In general, SCOPF problem is formulated as a constrained, nonlinear and non-convex optimization problem, which can be solved by either conventional gradient-based approaches (e.g.

Newton-Raphson method, interior point algorithm, etc.), or by non-conventional metaheuristic methods (e.g. evolutionary computation, swarm intelligence, etc.). Conventional SCOPF methods solve corresponding nonlinear equations using gradient-based iterative approaches and are formulated in a computationally efficient manner, but are sensitive to the initial values, might suffer from convergency problems and require the objective function to be differentiable. On the other hand, metaheuristic methods are based on some guided-search and stochastic rules, i.e. they perform guided random search over the problem space and handle constraints by formulating suitable penalty functions. Although metaheuristic optimization methods usually require (much) longer computational times due to a repetitive evaluation of the objective function, they do not suffer from convergency problems and are much less sensitive to the selection of initial values. Finally, conventional SCOPF methods are regularly used by network planners and operators, while none of the metaheuristic methods has seen implementation in power industry, even for off-line analysis of electrical networks during both design and planning stages.

When the network is overstressed with severe multiple contingencies, conventional SCOPF methods may fail to provide a solution due to the two main reasons: a) it is impossible to assume the proper initial values, as the system is far away from the pre-contingency conditions and all previously known operating points, and b) the problem may become overconstrained, or the underlying matrices cannot be solved numerically. The non-convergency of the conventional OPF algorithms due to problem infeasibility is more common [3] and is one of the most under-addressed issues in power systems analysis [4]. Nevertheless, the network operators need to identify the critical constraint violations causing those convergency problems, in order to devise optimal post-contingency corrective control actions (e.g. load shedding) to maintain the security and preserve the network integrity.

Building on the previous work in [5]-[8], this paper demonstrates how metaheuristic SCOPF methods with a suitable penalty constraint handling can: a) provide solution when conventional methods fail to converge, b) identify the critical constraint violations and provide solution in which all

other (except these critical) constraints will be satisfied by adjusting primary controls, c) help to evaluate critical constraints in terms of “available response time” for the activation of the secondary controls, i.e. introduce time-constrained SCOPF analysis, and d) specify the most effective corrective post-contingency actions, e.g. in terms of minimum load shedding, or activation of minimum capacity reserve.

## II. SECURITY CONSTRAINED OPTIMAL POWER FLOW

The SCOPF analysis aims to find the optimal settings of primary control variables (generator outputs, reactive power compensation, voltage set points, etc.), in order to minimize one or more objective functions, separately or simultaneously, while satisfying all specified equality and inequality constraints, either during the normal operating conditions, or for devising the suitable post-contingency corrective actions.

The OPF/SCOPF problem can be formulated as:

$$\min. f(x_0, u_0) \quad (1)$$

$$s.t. g(x_c, u_0) = 0 \quad (2)$$

$$h(x_c, u_0) \leq 0, c \in C = \{0, 1, 2, \dots, N_c\} \quad (3)$$

where:  $x, u$ : state and control variables,  $c$ : contingency index (zero for base case),  $C$ : set of considered contingencies.

Different formulations of SCOPF problem can include various objective functions,  $f$ , to meet various technical, economic and other (e.g. environmental) requirements. In this paper, two frequently used objective functions: fuel cost and active power loss are optimized separately [5]. Equality constraints,  $g$ , are represented by the power balance equations, while inequality constraints,  $h$ , represent equipment operating limits: generator active and reactive power limits, transformer tap setting limits, bus voltage limits, line loading limits, etc.

### A. Implemented SCOPF Algorithms

Two conventional algorithms (“IPA” and “PSSE”), and one metaheuristic algorithm (particle swarm optimization, “PSO”), are used in the presented analysis. Detailed description of the conventional solvers is given in [9]-[10], while implementation of PSO for SCOPF analysis is available in [11].

### B. Identification of Critical Constraints

Metaheuristic algorithms belong to a class of direct search methods, which use penalized objective function values to guide stochastic search process. The difference between the penalized function value (PFV) and original function value (OFV) is an indication of the severity of solution infeasibility: the greater the difference, the higher the number (and extent) of constraint violations. As the iterations progress, the search will either lead to zero measure of violation (all constraints are satisfied), resulting in the convergence of the original constrained problem, or, if there is no solution satisfying all constraints, PFV will be used to minimize the number still unresolved constraint violations. These remaining constraint violations, denoted as “critical constraints”, are the main cause of the solution infeasibility, as they cannot be resolved with primary control variables, i.e. within their allowed ranges

of variations. Critical constraints can be resolved only if additional secondary controls are applied (e.g. load shedding) and information on critical constraints can be used to help devising the most effective corrective actions.

## III. SELECTION OF SUITABLE PENALIZATION APPROACH

In their original form, search-based optimization algorithms can be applied only to unconstrained problems. Accordingly, constrained optimization problems should be converted to the unconstrained ones, using either interior or exterior penalty functions. Selection of a suitable penalization of the constrained infeasible solutions is very important, as the performance of an optimization algorithm often critically depends on the implemented constraint handling approach. Most of the exterior penalty functions are defined as problem-independent (especially in metaheuristic algorithms) and therefore may guide solution to a sub-optimal, or infeasible region. This is more likely to happen when the search space is limited, as in the case of multiple contingencies, when finding a feasible solution is difficult, or even impossible.

In order to demonstrate how an improved and more efficient penalization approach can be applied in the SCOPF studies (in terms of both guiding the search and finding the best practical solution), this section compares three widely used problem-independent approaches, revises one problem-dependent approach previously proposed by the authors in [8] and introduces one novel problem-dependent approach.

A generalized form of penalized objective function,  $f_p$ , is given by (4), representing modification (i.e. “penalization”) of the original objective function,  $f$ , where one penalty functions is defined for the violation of equality constraints,  $\phi_{eq}$ , and another for the violation of inequality constraints,  $\phi_{ineq}$ . Both penalty functions can be specified in different ways, e.g. as the problem-dependent/independent numerical interpretations of the evaluated extent of the specific constraint violation.

$$f_p(x, u) = f(x, u) + \phi_{eq}(g(x, u)) + \phi_{ineq}(h(x, u)) \quad (4)$$

### A. Problem-Independent Penalty Functions

The three most commonly used problem-independent penalty functions are specified by the corresponding penalty coefficients,  $K_{eq}$  and  $K_{ineq}$ , as the constant, linear and quadratic terms in (5)-(6), (7)-(8) and (9)-(10), respectively.

#### 1) Constant penalty function (CPF):

$$\phi_{eq}(g(x, u)) = \begin{cases} 0 & \text{if } g(x, u) = 0 \\ \sum_{i=1}^{N_{eq}} K_{eq,i} & \text{if } g(x, u) \neq 0 \end{cases} \quad (5)$$

$$\phi_{ineq}(h(x, u)) = \begin{cases} 0 & \text{if } h(x, u) \leq 0 \\ \sum_{i=1}^{N_{ineq}} K_{ineq,i} & \text{otherwise} \end{cases} \quad (6)$$

#### 2) Linear penalty function (LPF):

$$\phi_{eq}(g(x, u)) = \sum_{i=1}^{N_{eq}} K_{eq,i} * |g_i(x, u)| \quad (7)$$

$$\phi_{ineq}(h(x, u)) = \sum_{i=1}^{N_{ineq}} K_{ineq,i} * \max(0, h_i(x, u)) \quad (8)$$

3) Quadratic penalty function (QPF):

$$\phi_{eq}(g(x, u)) = \sum_{i=1}^{N_{eq}} K_{eq,i} * |g_i(x, u)|^2 \quad (9)$$

$$\phi_{ineq}(h(x, u)) = \sum_{i=1}^{N_{ineq}} K_{ineq,i} * (\max(0, h_i(x, u)))^2 \quad (10)$$

B. Problem-Dependent Penalty Functions

In general, problem-dependent penalization approaches require longer computational times for the correct evaluation of penalty factors, but provide a more realistic solution, as they more accurately represent the specific constraint violation conditions. The application of the two such approaches in SCOPF analysis is discussed in the further text.

1) Assessment of thermal loading limits of overhead lines: Thermal loading limits of overhead lines are an important physical constraint that has to be considered during the power system analysis. Excessively high temperatures might result in the elongation and sagging of conductors, i.e. reduced safety clearance distances, as well as in the conductor annealing. In order to prevent damage and safety hazards, overhead line conductors should operate with the currents that will prevent thermal overloading, usually expressed in terms of “ampacity”. The relationship between the ampacity of a conductor,  $I$ , and the conductor’s surface temperature,  $T_c$ , can be calculated by a heat balance equation, (11) [12].

$$q_c + q_r + mC_p \frac{dT_c}{dt} = q_s + I^2 R(T_c) \quad (11)$$

where:  $q_c$  and  $q_r$  are the heat losses due to convection and radiation,  $q_s$  and  $I^2 R(T_c)$  are the heat gains due to solar radiation and flow of current  $I$ , respectively, and  $mC_p$  is the thermal capacity of the conductor.

Assuming the steady state operating conditions before the contingency has occurred (when derivative  $dT_c/dt$  is zero), the pre-contingency conductor temperature is determined by the pre-contingency current for assumed ambient conditions (e.g. these in [12]). The relationship between the conductor temperature and its current is illustrated in Fig. 1 using as example standard ACSR conductor from [13] (“Sparrow 6/1”).

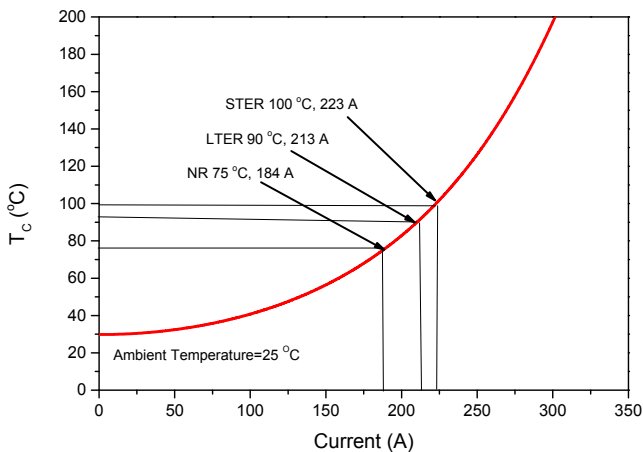


Fig. 1. Equilibrium conductor temperature,  $T_c$ , as a function of its current, [12]

If the post-contingency current is higher than the pre-contingency current, the conductor temperature will start to increase according to (11), based on the pre-contingency current/temperature and assumed ambient conditions. Upon reaching the set limit for the maximum allowed temperature, thermal protection will be activated. The time required for the activation of protection during the post-contingency is denoted as the allowed overloading time (OVT). Fig. 2 illustrates OVT calculation based on the maximum allowed conductor temperature of 100° C and pre-contingency temperature of 40° C (corresponding to a pre-contingency current of  $I_0=100$  A). Three post-contingency currents are illustrated:  $I_1=250$  A,  $I_2=218$  A and  $I_3=150$  A, which would result in the three final temperatures of  $T_{cf1}=126.4^\circ$  C,  $T_{cf2}=96.0^\circ$  C and  $T_{cf3}=56.4^\circ$  C, respectively. In the case of the post-contingency current  $I_1$ , the thermal protection will react when conductor’s temperature reaches 100° C, giving OVT<sub>1</sub> value of about 4min.

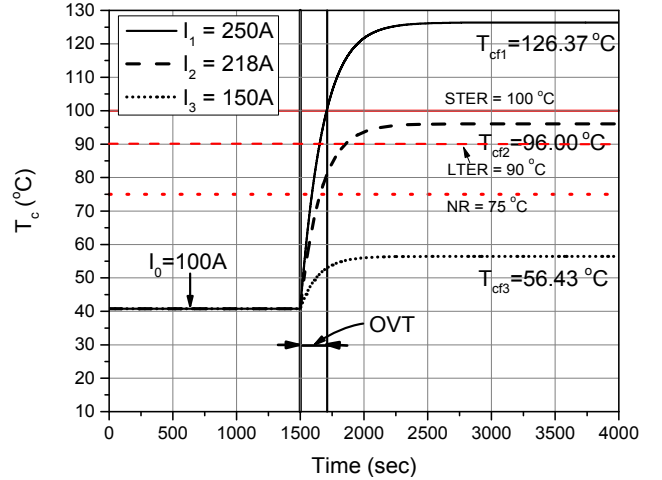


Fig.2. Illustration of the calculation of allowed overloading time (OVT)

As the tripping of any overloaded line will only worsen the post-contingency operating conditions, the minimum OVT of all overloaded lines represents the time available for devising appropriate corrective actions by network operators. In other words, the SCOPF algorithm will search amongst all possible post-contingency system states and if there is no feasible solution satisfying all line loading constraints (i.e. if there is one or more critical line loading constraints), the penalization based on the OVT values will produce the minimum PFV, which will allow to select the solution with the settings of the primary controls that will provide network operator with the longest time for deciding on the most effective secondary controls (e.g. load shedding), in order to return the network into the feasible operating region.

To the best of the authors’ knowledge, the described penalization approach allows to introduce, for the first time, “time-constrained SCOPF analysis”, in which optimal solution obtained by OVT-based penalization does not minimize the number of constraint violations, but instead maximizes the time available to network operator for devising the suitable post-contingency corrective actions.

2) *Piecewise penalty function (PPF)*: As discussed, the allowed time (OVT) for which an overloaded line can be operated in the post-contingency conditions is determined by the amount of the increased current/power flow, i.e. the severity of the violated line loading constraint. If the impact of ambient conditions and transient process of the dynamic changes of conductor temperature during the post-contingency period is neglected, the first approximation for the evaluation of the line overloading conditions can be done using Fig. 1 and defining the three following temperature-current ratings: a) normal rating (NR) when conductor temperature is below 75° C, b) long-term emergency rating (LTER), when conductor temperature is between 75° C and 90° C, and c) short-term emergency rating (STER), when conductor temperature is between 90° C and 100° C [14], [15].

In terms of the time for which a line can be operated in overloaded conditions, one STER violation is more severe (i.e. gives a shorter available time for managing critical post-contingency constraints) than several LTER violations (which can be tolerated for longer times). Accordingly, penalization of objective function formulated using piecewise penalty factors can be written as:

$$\phi_{PF} = \begin{cases} 0 & \text{if } PF \leq NR \\ K_1 & \text{if } NR < PF \leq LTER \\ K_2 & \text{if } LTER < PF \leq STER \\ K_3 & \text{if } PF > STER \end{cases} \quad (12)$$

where:  $PF$  is the actual line current (or MVA flow) and  $K_1$ ,  $K_2$  and  $K_3$  are the penalty factors ( $K_1 \ll K_2 \ll K_3$ ), Table I.

TABLE I. SELECTION OF PIECEWISE PENALTY FACTORS

PARAMETER	RATING		
	NR	LTER	STER
Temperature (° C)	75	90	100
Current (A)	189	210	223
Current (% of rated)	100	111	118
Piecewise Penalty Factors	$K_1$ NR < PF ≤ LTER	$K_2$ LTER < PF ≤ STER	$K_3$ PF > STER
Fuel Cost	500	5,000	10,000
Active Power Loss	500	5,000	10,000

3) *Dynamic penalty function (DPF)*: Dynamic (thermal rating) penalty function considers the actual OVT values of all post-contingency overloaded lines, which are determined by (11) and with reference to Fig. 2. The calculation of OVT values is illustrated in Fig. 3, where different curves represent different pre-contingency currents, while post-contingency currents that determine the corresponding OVT values on Y-axis are given on X-axis.

For the used conductor example from [13], the thermal rating for the continuous operation (i.e. normal rating, NR) is 75° C, while rating for emergency operation (also set as the maximum temperature before protection trips the line) is 100° C. Assuming no control action is implemented in the post-contingency state, the distinction is made between the following two conditions: a) if the final temperature is over 75° C, but below 100° C, the penalty is applied according to

the final temperature (Fig. 2,  $I_2=218A$ ); b) if the final temperature is higher than 100° C (Fig. 2,  $I_1=250A$ ), the penalty is determined by the corresponding OVT value (Fig. 3). The two related penalty functions and penalty factors are given by:

$$\phi_{PF} = \begin{cases} \frac{K_1(T_{cf}-50)}{25} & \text{if } 75^\circ\text{C} < T_{cf} \leq 100^\circ\text{C} \\ \frac{K_2}{OVT} & \text{if } T_{cf} \geq 100^\circ\text{C} \end{cases} \quad (13)$$

where:  $K_1$  is set as 500 and  $K_2$  as 5,000,000.

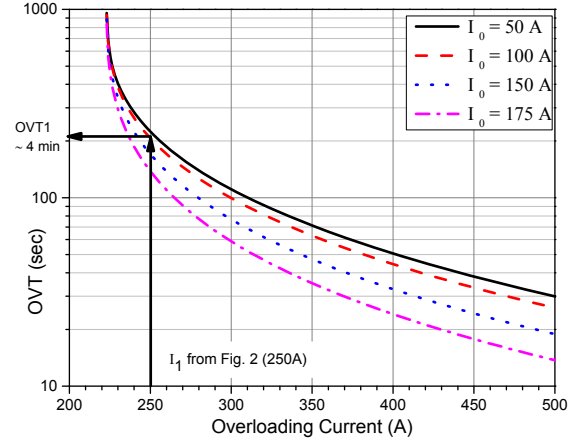


Fig. 3. Calculation of OVT: Different curves correspond to different pre-contingency currents, while post-contingency currents are on X-axis

#### IV. TEST NETWORK USED FOR ANALYSIS

The test network selected for the analysis is a widely-used IEEE 14-bus network, Fig. 4, which is N-1 contingency-constrained network. The network has five generators and 11 load points, with total active and reactive power demands of 259 MW and 73.50 MVar, respectively. Loads are assumed to be “constant power” type, tap settings of transformers are assumed as fixed and allowed range of variations of bus voltages is assumed as  $\pm 10\%$  of the nominal value. The detailed information on network can be found in [16].

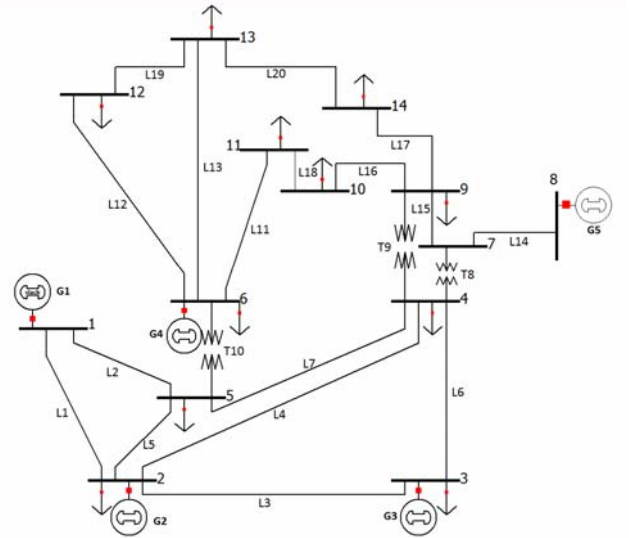


Fig. 4. IEEE 14-bus test network [16]

## V. RESULTS AND DISCUSSION

The results presented in this section compare performance of two conventional SCOPF solvers (interior point algorithm, IPA, and PSSE) and one metaheuristic algorithm (PSO) with five different penalty functions in solving feasible and infeasible SCOPF cases. One single-line contingency (i.e. outage of line L1-2) and two double-line contingencies (i.e. outages of lines L4-9&L6-13, and L6-13&L9-14), are analysed for the two pre-contingency optimal operating points, resulting in both feasible (single-line contingency) and infeasible (double-line contingencies) SCOPF cases.

### A. Feasible SCOPF Cases

The single-line contingency case has no critical constraint violations, which means that conventional methods can converge and find feasible optimal solution for both considered objective functions (cost and active power loss minimization) with zero constraint violations, Table II. For this feasible case, all PSO algorithms (with different penalty functions) provide solutions either close to those with the two conventional algorithms, or better, clearly demonstrating applicability of metaheuristic methods for SCOPF studies.

TABLE II. OBJECTIVE FUNCTION VALUES WITH CONVERGENCY STATUS

Contingency	Conventional		PSO				
	IPA	PSSE	CPF	LPF	QPF	PPF	DPF
<i>Fuel Cost Minimization</i>							
L1-2	863.6	862.5	865.5	864.6	864.0	865.71	867.72
L4-9 & L6-13	X	X	801.93	799.5	797.8	786.60	805.11
L6-13 & L9-14	X	X	813.0	809.6	809.2	791.70	797.45
<i>Active Power Loss Minimization</i>							
L1-2	1.254	1.243	1.249	1.245	1.249	1.179	1.179
L4-9 & L6-13	X	X	2.422	2.499	2.575	2.395	3.202
L6-13 & L9-14	X	X	5.720	5.715	5.716	5.665	5.662

X Denotes inability to converge

### B. Infeasible SCOPF Cases

For the two double-contingency cases, both conventional methods fail to converge (indicated by "X" in Table II). For these cases, the PSO-based SCOPF algorithm with different penalty functions can converge, as the penalized solutions (PFV) with minimized number/amount of constraint violations are accepted as the optimal solutions. It can be seen that DPF-based PSO solution for contingency L4-9&L6-13 and loss minimization is higher than the other four PSO solutions, as DPF solution provides PFV with significantly longer OVT, but higher objective function (further illustrated in Table IV). For contingency L6-13&L9-14, all five PSO solutions in Table II are close, as are the OVT values in Table V.

In order to understand why conventional methods failed to converge and what are the benefits of different penalization approaches for metaheuristic method, Table III lists constraint violations in the immediate post-contingency state, obtained by solving an unconstrained Newton-Raphson power flow, (UCPF) with the pre-contingency optimal control set points still applied on the reconfigured post-contingency network (after the protection system clears the faults).

TABLE III. LIST OF IMMEDIATE POST-CONTINGENCY CONSTRAINT VIOLATIONS (BEFORE IMPLEMENTING SCOPF ANALYSIS)

Contingency	Bus Undervoltage (UV) Constraint Violations		Line Overloading (OL) Constraint Violations	
	Number	Index	Number	Index
	L1-2	0	/	3
L4-9&L6-13	0	/	4	L2-3, L4-5, L7-9, L12-13
L6-13 & L9-14	2	B13, B14	6	L2-3, L4-5, L5-6, L6-12, L12-13, L13-14

The PSO-based SCOPF solutions can reduce the number of post-contingency constraint violations from Table III to only the critical constraints, which are the main reason for the non-convergence of conventional algorithms. This is illustrated in Tables IV and V, which list the number of critical constraint violations identified by PSO algorithm with different penalizations. These results are PFV outputs, as the solution satisfying all constraints with available primary controls is not possible, indicating that the secondary controls should be applied (discussed in the next section).

Although the number of critical constraints identified by PSO-based SCOPF with different penalty functions in Tables IV and V is lower than the number of constraints in Table III, there are important differences in the results from the different penalization approaches. The number of the identified critical constraints ranges from two to five, with additional differences in the calculated OVT values (the longest with DPF), which demonstrate importance of selecting a suitable penalization approach for metaheuristic methods.

TABLE IV. PSO SCOPF LIST OF IDENTIFIED CRITICAL CONSTRAINTS WITH DIFFERENT PENALTY FUNCTIONS (CONTINGENCY L4-9 & L6-13)

Applied Penalty	Critical OL Constraints	Critical UV Constraints	OVT (s)
<i>Fuel Cost Minimization</i>			
CPF	L7-9, L12-13	/	400.34
LPF	L7-9, L12-13	/	522.48
QPF	L2-3, L6-11, L7-9, L10-11, L12-13	/	281.7
PPF	L2-3, L7-9, L12-13	/	487.4
DPF	L7-9, L12-13	/	1369.24
<i>Active Power Loss Minimization</i>			
CPF	L7-9, L12-13	/	112.48
LPF	L7-9, L12-13	/	526.26
QPF	L7-9, L10-11, L12-13	/	281.58
PPF	L7-9, L12-13	/	368.48
DPF	L7-9, L12-13	/	1324.2

TABLE V. PSO SCOPF LIST OF CRITICAL CONSTRAINTS WITH DIFFERENT PENALTY FUNCTIONS (CONTINGENCY L6-13&L9-14)

Applied Penalty	Critical OL Constraints	Critical UV Constraints	OVT (s)
<i>Fuel Cost Minimization</i>			
CPF	L6-12, L12-13, L13-14	B13, B14	27.42
LPF	L6-12, L12-13, L13-14	B13, B14	32.62
QPF	L6-12, L12-13, L13-14	B13, B14	32.62
PPF	L6-12, L12-13, L13-14	B13, B14	32.62
DPF	L6-12, L12-13, L13-14	B13, B14	32.62
<i>Active Power Loss Minimization</i>			
CPF	L6-12, L12-13, L13-14	B13, B14	32.58
LPF	L6-12, L12-13, L13-14	B13, B14	32.58
QPF	L6-12, L12-13, L13-14	B13, B14	32.58
PPF	L6-12, L12-13, L13-14	B13, B14	32.58
DPF	L6-12, L12-13, L13-14	B13, B14	32.58

The main reasons for the differences in the numbers of the identified critical constraints and corresponding OVT with the PSO-based method are: a) the two different pre-contingency temperatures (for two different pre-contingency operating points, corresponding to the minimization of costs and minimization of active power losses) are correctly acknowledged with the PPF and DPF penalization approaches (problem-dependent) and ignored with the CPF, LPF and QPF approaches (problem-independent), b) the longest OVT values are most accurately calculated with the DPF approach, and c) the penalized PSO SCOPF solutions (i.e. PFVs) differ in terms of the actually achieved line loading conditions. This is illustrated in Figs. 5 and 6, showing the line loadings for unconstrained power flow solution and five PSO SCOPF solutions with different penalty functions. The DPF solution provides the minimum number/amount of critical constraints (lines L7-9 and L12-13 in Fig. 5 and lines L6-12, L12-13, L13-14 in Fig. 6), i.e. the longest OVT for the network operators to consider the most efficient corrective actions.

### C. Constraint Relaxation in Conventional SCOPF Methods

In order to aid convergency of conventional methods and in that way identify critical constraints, all security constraints are in this section treated as “soft constraints” and modelled using linear and quadratic exterior penalty functions. The list of resulting constraint violations for the final solutions with various penalty factor ( $K_p$ ) values is shown in Table VI.

The purpose of relaxing constraints in the conventional method is to widen the search space by allowing the infeasible region to become feasible, so there is a much higher degree of freedom during the search. However, this approach in all cases results in a higher number of identified critical constraints, as compared to metaheuristic algorithm (Tables IV and V).

TABLE VI. LIST OF CONSTRAINT VIOLATIONS WITH VARIOUS PENALTIES FOR SOFT CONSTRAINT HANDLING (PSSE ALGORITHM)

Type of penalty function	Linear Penalty			Quadratic penalty		
	$K_p \rightarrow$	10	100	1000	10	100
<b>Fuel Cost Minimization, Contingency L4-9 &amp; L6-13</b>						
Bus Voltage Violations	5	0	0	14	0	0
Line MVA violations	4	4	4	4	4	4
<b>Fuel Cost Minimization, Contingency L6-13 &amp; L9-14</b>						
Bus Voltage Violations	11	4	4	14	142	2
Line MVA violations	4	4	3	4	3	4
<b>Active Power Loss Minimization, Contingency L4-9 &amp; L6-13</b>						
Bus Voltage Violations	0	0	0	0	0	0
Line MVA violations	5	5	5	5	5	5
<b>Active Power Loss Minimization, Contingency L6-13 &amp; L9-14</b>						
Bus Voltage Violations	4	3	3	7	3	2
Line MVA violations	4	4	4	4	3	4

Based on the comparison of results in Tables IV, V and VI, it can be seen that conventional methods can converge after a penalization is applied, but the number (and index) of constraints that should be relaxed in the final solution varies for different applied exterior penalty functions and penalty values (with no general rule. It is also found that the index of relaxed constraints in conventional methods varies for different initial conditions and in multiple runs.

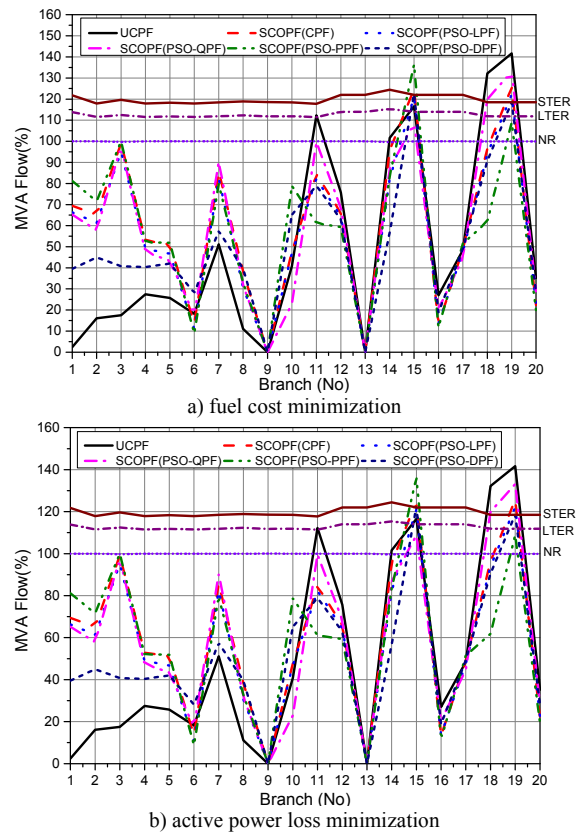


Fig. 5. Line MVA flows for unconstrained power flow solution and five PSO solutions with different penalty functions (contingency L4-9 and L6-13)

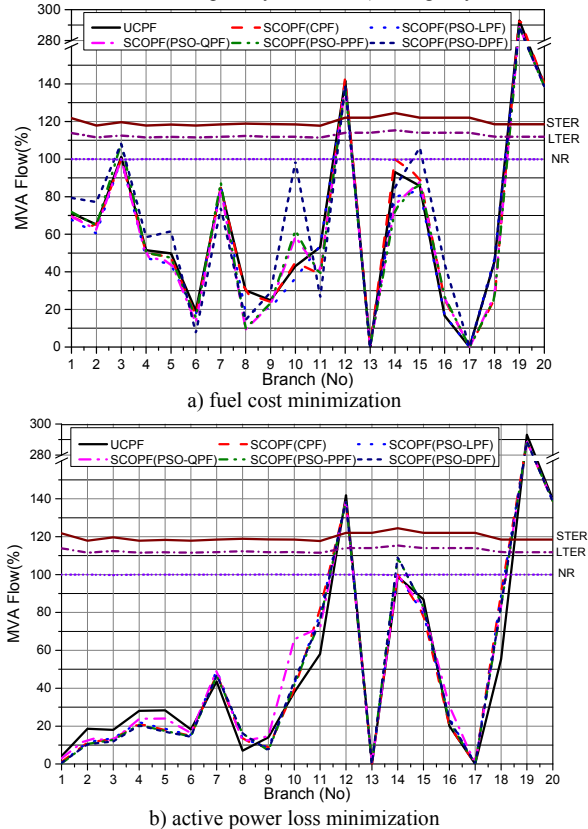


Fig. 6. Line MVA flows for unconstrained power flow solution and five PSO solutions with different penalty functions (contingency L6-13 and L9-14)

The following observations can be made from the results presented in this section:

- For the feasible SCOPF case, both conventional and metaheuristic algorithms converge and provide similar solutions for two used objective functions, satisfying all constraints. Conventional methods are generally better for analysis of feasible cases, as they are computationally more efficient, requiring only a few seconds on a standard desktop PC to provide the solution (if they can converge), while PSO method requires a few minutes of computational time.
- For the infeasible SCOPF cases, conventional methods fail to converge, but PSO methods with penalization can converge and can identify the critical constraints, which are the actual causes of the convergence problems. This demonstrates an important advantage of metaheuristic methods, as even after soft constraint handling is applied in conventional methods to aid their convergence, the number of unresolved critical constraints is still higher than in metaheuristic methods.
- The PSO solutions with different penalty functions are different, but DPF penalization approach ensures SCOPF solutions that provide network operators with the longest time for devising corrective actions.

## VI. COMPARISON OF DIFFERENT LOAD SHEDDING APPROACHES

This section discusses how the information on the minimum number and extent of critical constraint violations, which can be identified by PSO-based method with a realistic representation of line dynamic loading (DPF) in post-contingency stage, can be used to help the convergence of the conventional SCOPF methods. In other words, PSO SCOPF with DPF indicates the minimum number of constraints that should be relaxed to allow conventional algorithms to converge and therefore offers a more efficient alternative to soft constraint handling. Furthermore, the information on the minimum number and extent of critical constraint violations can be used to devise the most effective corrective actions in terms of the applied secondary controls for returning the system into the feasible operating region.

The PSO SCOPF method with DPF has identified lines L7-9 and L12-13 as the critical constraints for one double-contingency (simultaneous faults of lines L4-9 and L6-13) and lines L6-12, L12-13 and L13-14 as the critical constraints for another contingency (simultaneous faults of lines L6-13 and L9-14) for both pre-contingency operating conditions, Tables IV and V. As the post-contingency overloading conditions of these “critical lines” cannot be resolved with available primary controls (e.g. by re-dispatching and changing outputs of the generators, or by re-adjustment of volt-var controls), the secondary controls should be activated to prevent further tripping of the overloaded lines. These secondary controls are part of system support services, including, e.g. connection of reserve generation capacity, or disconnection of system loads, also known as “load shedding”.

In the context of “smart grid” applications, demand side management (DSM) functionalities have recently emerged as an alternative to load shedding, as DSM can easily provide required reduction in demand over the periods as long as a few hours, i.e. until the system can provide enough generation and transfer capacity to meet all demand (including activated DSM loads that should be re-connected). Essentially, both DSM and load shedding provide the same system support functionality—reduction of system load—although there might be significant differences in the targeted types of loads, in required control and management infrastructures and in actual arrangements for the provision of the related system support services (e.g. the “balancing mechanism” in the UK, [18]). Accordingly, although this paper considers only load shedding as the secondary control activated for reducing demands and resolving the post-contingency line overloading, DSM can be also used for the same purpose (this is the subject of the further work by the authors).

The selection of the target buses for the application of load shedding generally depends on the locations and proportions of sheddable loads. In the context of the analysis in this paper, however, it is assumed that all load buses are available for load shedding and that loads can be shed in any desired amount, up to the total connected load. Accordingly, the three load shedding approaches are analysed in this section: a) hard load shedding (HLS), b) optimal load shedding (OLS), and c) selective optimal load shedding (SOLS).

The target buses for both HLS and OLS approaches are the buses associated with the immediate post-contingency constraint violations calculated with the unconstrained power flow solutions, Table III. In the HLS approach, the total load at these target buses is disconnected (100% load shedding at target buses). In the OLS approach, the loads at the target buses are considered as the control/search variables during the SCOPF analysis, which helps to optimize load shedding (resulting in 0%-100% load shedding at target buses). The target buses for SOLS approach are selected as the buses with the highest absolute “injection sensitivity factors” (ISFs) with respect to critical line overloading constraints, as the power flows in the critical lines are most influenced by the power injections at these buses. Again, the loads at these most sensitive buses are considered as control variables during the SCOPF analysis, which also resulted in the optimization of the load shedding (0%-100% load shedding at the buses with the highest ISFs with respect to the critical line overloadings).

### A. SOLS Algorithm

The SOLS-based SCOPF analysis for resolving post-contingency infeasible cases can be formulated as an algorithm with the following steps:

- 1) Select the infeasible SCOPF cases for which conventional algorithms fail to provide solution;
- 2) Solve the considered case with a suitable metaheuristic algorithm and identify minimum number/extent of critical constraint violations for that solution (e.g. PSO with DPF);

- 3) Calculate ISFs for all buses with respect to the critical overloaded lines (see next section);
- 4) Identify buses with the highest absolute ISF values and input loads at these buses as the control variables during the SCOPF analysis;
- 5) Using a suitable conventional or metaheuristic algorithm, solve the modified SCOPF problem, with a new objective function: minimizing the amount of load that should be disconnected at target buses in Step 4, in order to provide solution with zero constraint violations.

#### B. Calculation of Injection Sensitivity Factors (ISFs)

Calculation of ISFs quantifies the redistribution of power flows through all network lines due to a change of generation or load (positive or negative “injected power”) connected at a specific bus, with slack bus constraint included. Essentially, the ISF captures the sensitivity of the power flow through a line with respect to the changes in the power injection (i.e. connected generation or load) at a considered bus [15]. General ISF expression for a line between buses  $i$  and  $j$ , with respect to the power injection at bus  $k$ , can be written as:

$$ISF_{ij}^k = \frac{\partial P_{ij}}{\partial P_k} = \frac{\Delta P_{ij}^k}{\Delta P_k}; k \in B \text{ and } (ij) \in L \quad (14)$$

where:  $B$ -bus index;  $L$ - line index;  $\Delta P_k$ -change in active power injection at bus  $k$ ;  $\Delta P_{ij}^k$ -change in active power flow in line  $(i, j)$  due to a change in power at the bus  $k$ ,  $\Delta P_k$ .

#### C. Comparison of Different Load Shedding Approaches

The results of different load shedding approaches are compared for the two previously considered double-line contingencies: a) simultaneous outage of lines L4-9 and L6-13 and b) simultaneous outage of lines L6-13 and L9-14.. Table VII lists ISFs for these critical lines and all network buses, while Table VIII lists buses selected for different load shedding approaches.

TABLE VII. INJECTION SENSITIVITY FACTORS

Bus	Contingency: L4-9 & L6-13		Contingency: L6-13 & L9-14		
	L7-9	L12-13	L6-12	L12-13	L13-14
Bus 1	0.235	0.257	0.000	0.000	0.000
Bus 2	0.224	0.064	0.000	0.000	0.000
Bus 3	0.035	0.001	0.000	0.000	0.000
Bus 4	0.015	0.000	-0.007	-0.004	-0.001
Bus 5	0.004	-0.001	-0.008	-0.005	-0.001
Bus 6	0.000	-0.004	-0.018	-0.010	-0.002
Bus 7	-0.006	-0.007	-0.005	-0.003	-0.001
Bus 8	-0.221	-0.012	-0.003	-0.002	0.000
Bus 9	-0.322	-0.066	-0.006	-0.003	-0.001
Bus 10	-0.397	-0.071	-0.009	-0.005	-0.001
Bus 11	-0.444	-0.077	-0.013	-0.007	-0.002
Bus 12	-0.568	-0.106	-1.182	-0.056	-0.013
Bus 13	-0.570	-0.316	-1.598	-1.282	-0.032
Bus 14	-0.639	-0.571	-1.918	-1.524	-1.120

TABLE VIII. TARGET BUSES FOR CONSIDERED LOAD SHEDDING APPROACHES

Type of Load Shedding	Contingency: L4-9 and L6-13	Contingency: L6-13 & L9-14
HLS	1,2,3,4,5,6,7,9,12, 13	2,3,4,5,6,12,13,14
OLS	1,2,3,4,5,6,7,9,12, 13	2,3,4,5,6, 12,13,14
SOLS	13, 14	13, 14

While all buses associated with immediate post-contingency constraint violations (Table III) are considered as target buses for HLS and OLS, only two buses are considered for SOLS. It can be observed from the ISF values for the critical lines that power injections at Buses 13 and 14 have the highest impact on the power flows of overloaded critical lines. For example, for the outage of L6-13 and L9-14, the injection of 1 MW at Bus 14 will result in the reduction of 1.917 MW in power flow in line L6-12, 1.523 MW in line L12-13 and 1.119 MW in line L13-14. Accordingly, Buses 13 and 14 are considered as the target buses for SOLS. For different load shedding approaches and for conventional and PSO methods, the actual amount of the shed load is given in MWs and as the percentage of the total system load in Tables IX and X.

TABLE IX. LOAD SHEDDING IN MW AND IN PERCENTAGE OF SYSTEM CONNECTED LOAD (CONTINGENCY L4-9 & L6-13)

Type of Shedding	Conventional		PSO				
	IPA	PSSE	CPF	LPF	QPF	PPF	DPF
<b>Fuel Cost Minimization</b>							
HLS (MW)	231.60	231.60	231.60	231.60	231.60	231.60	231.60
(%)	89.421	89.421	89.421	89.421	89.421	89.421	89.421
OLS (MW)	194.70	194.40	204.76	204.77	204.91	204.68	204.66
(%)	75.174	75.058	79.058	79.060	79.116	79.029	79.021
SOLS(MW)	28.40	28.40	28.40	28.40	28.40	28.40	28.40
(%)	10.965	10.965	10.965	10.965	10.965	10.965	10.965
<b>Active Power Loss Minimization</b>							
HLS (MW)	231.60	231.60	231.60	231.60	231.60	231.60	231.60
(%)	89.421	89.421	89.421	89.421	89.421	89.421	89.421
OLS (MW)	131.8	177.95	157.25	117.07	160.51	147.73	103.28
(%)	50.88	68.707	60.714	45.200	61.793	57.040	39.877
SOLS(MW)	28.40	28.40	28.40	28.40	28.40	28.40	28.40
(%)	10.965	10.965	10.965	10.965	10.965	10.965	10.965
<b>Load Shedding Minimization</b>							
HLS (MW)	231.60	231.60	231.60	231.60	231.60	231.60	231.60
(%)	89.421	89.421	89.421	89.421	89.421	89.421	89.421
OLS (MW)	12.09	17.26	19.55	26.10	16.15	18.65	16.16
(%)	4.668	6.664	7.547	10.076	6.237	7.200	6.238
SOLS(MW)	12.00	28.36	13.81	12.96	12.28	9.28	9.04
(%)	4.633	10.950	5.232	5.003	4.739	3.584	3.490

TABLE X. LOAD SHEDDING IN MW AND IN PERCENTAGE OF SYSTEM CONNECTED LOAD (CONTINGENCY: L6-13 & L9-14)

Type of Shedding	Conventional		PSO				
	IPA	PSSE	CPF	LPF	QPF	PPF	DPF
<b>Fuel Cost Minimization</b>							
HLS (MW)	217.00	217.00	217.00	217.00	217.00	217.00	217.00
(%)	83.784	83.784	83.784	83.784	83.784	83.784	83.784
OLS (MW)	204.50	194.28	204.50	204.50	204.49	204.48	204.43
(%)	78.958	75.011	78.958	78.958	78.953	78.948	78.929
SOLS(MW)	28.40	28.40	28.40	28.40	28.40	28.40	28.40
(%)	10.965	10.965	10.965	10.965	10.965	10.965	10.965
<b>Active Power Loss Minimization</b>							
HLS (MW)	217.00	217.00	217.00	217.00	217.00	217.00	217.00
(%)	83.784	83.784	83.784	83.784	83.784	83.784	83.784
OLS (MW)	128.3	196.03	154.77	124.85	165.58	110.40	110.76
(%)	49.53	75.680	60.92	48.21	63.93	42.62	42.76
SOLS(MW)	28.40	28.40	28.40	28.40	28.40	28.40	28.40
(%)	10.965	10.965	10.965	10.965	10.965	10.965	10.965
<b>Load Shedding Minimization</b>							
HLS (MW)	217.00	217.00	217.00	217.00	217.00	217.00	217.00
(%)	83.784	83.784	83.784	83.784	83.784	83.784	83.784
OLS (MW)	17.60	17.61	17.65	17.71	17.71	17.54	17.06
(%)	6.795	6.798	6.816	6.836	6.839	6.771	6.588
SOLS(MW)	17.60	17.61	17.62	17.69	17.63	17.07	17.17
(%)	6.795	6.798	6.805	6.830	6.806	6.589	6.628

Based on the comparison of results for different load shedding approaches, the following observations can be made:

- Conventional algorithms can converge by controlling the load at target buses identified by PSO SCOPF method. In that way, metaheuristic algorithms can help convergency of the conventional SCOPF methods.
- The proposed SOLS approach, based on metaheuristic algorithm to identify minimum number/extent of critical constraints and corresponding calculated ISFs, provides lower load shedding than OLS and HLS (typically activated by the operator and/or protection systems).
- While the load shedding with minimizing active power losses leads to either equal or lower amount of shed load compared to the minimized fuel cost, minimizing load shedding always lead to a lower amount of shed load compared to the previous two.
- Although there are differences in the amount of shed load with different optimization objectives, the proposed SOLS approach seems to be the most efficient for returning the system into a feasible operating region (it results in the lowest line loadings, Fig. 7).
- For a given objective function, the proposed selective load shedding with dynamic penalty function will results in both equal or reduced amount of load shedding, compared to conventional and PSO with other penalty functions.

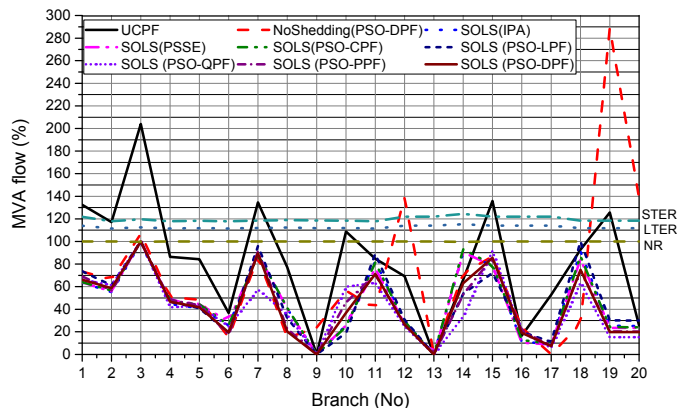


Fig. 7. Line MVA flows with and without load shedding for fuel cost minimization (contingency L6-13 and L9-14)

## VII. CONCLUSIONS

The development and implementation of the accurate, robust, flexible and computationally efficient analytical and modelling tools is very important for ensuring optimal design and secure operation of power supply systems, which are even more relevant in the context of the anticipated transformation of existing electricity networks into the future “smart grids”. Optimal power flow (OPF) and security-constrained OPF (SCOPF) are amongst the most frequently used tools for the evaluation of performance of electricity networks at both planning and operational stages. In that context, particularly important are “smart grid” applications requiring real time control of large interconnected power supply systems,

especially when multiple severe contingency occur. In such cases, network operators face two considerable challenges: a) time available for devising appropriate corrective actions for returning the system into a feasible operating region is typically (very) limited, and b) conventional SCOPF methods might fail to converge and provide solution due to a high number of post-contingency constraint violations (when “soft” constraint handling and repetitive constraint relaxation are difficult to implement), or conventional SCOPF methods might diverge due to the inability to select proper initial values (the system is far away from pre-contingency operating conditions and all previously known operating points).

This paper demonstrates how one metaheuristic SCOPF method, particle swarm optimization, PSO, with a suitable penalty constraint handling, based on a novel formulation of “dynamic penalty function”, DPF, can identify minimum number and extent of critical constraint violations and provide solution when conventional SCOPF methods fail to converge. These critical constraints are the actual causes of infeasibility in the conventional SCOPF problem, as they cannot be resolved with the allowed ranges of variations of all available primary control variables.

Further evaluation of severity of critical constraints, i.e. post-contingency line overloadings in terms of “available response time” before the thermal protection disconnects the overloaded lines, allowed to establish “time-constrained SCOPF analysis”, which, to the best knowledge of the authors, for the first time introduces in the system security (SCOPF) analysis evaluation (and calculation) of the time available to network operators for devising appropriate corrective actions for returning the system into a feasible operating region.

As the post-contingency critical constraints can be resolved only by activating secondary controls, information on critical constraints obtained by PSO-based SCOPF with DPF penalization (i.e. identification of the minimum number/extent of critical constraint violations) is used during the second part of the presented analysis, in order to select the most effective corrective actions, illustrated on the example of load shedding. Three different load shedding approaches are compared, where one of them, i.e. selective optimal load shedding, SOLS, based on the calculation of injection sensitivity factors, ISFs, allowed to select only a very few buses with the highest impact on the overloaded lines and, in that way, devise the minimum load shedding strategies.

The ISF-based corrective controls and responsive actions are particularly promising for “smart grid” applications with highly dispersed distributed generation and demand-manageable load resources, as they generally allow to evaluate individual contributions from available controllable units at network buses (Table VII) and then devise the optimum control schemes, e.g. SOLS, capable of maximizing system support benefits from decentralised ancillary services, while minimizing possible negative impact on customers.

It should be noted that conventional SCOPF methods require much shorter computational times to provide solution (in order of seconds), in comparison to metaheuristic SCOPF methods (in order of minutes). This increase of computational time is a significant disadvantage of metaheuristic methods, particularly for the analysis of large interconnected networks, which, however, can be overcome by implementing inherent task-level parallelism at objective function calculation stage and data-level parallelism at optimization stage. Furthermore, handling of a typically high number of constraint violations in post-contingency stage by metaheuristic algorithms can be addressed by developing domain-independent constraint handling approaches. This is also subject of the further work by the authors.

In a more general context, the increased numbers of various wide area measurement (WAM) and SCADA monitoring systems and technologies now provide network operators with a more detailed and more accurate (real time, or close to real time) information on the network configurations, operating and loading conditions and states of the network components and relevant control, protection and management settings and parameters. This allows to use the presented SCOPF-based analysis as either part of existing automatic control tools, or to implement SCOPF for a fully independent automatic control in dispatching/operating centres, rather than only for the traditional studying and evaluation of system performance. In that context, this paper presented analysis where some existing automatic control and protection systems that will be activated in post-contingency operating state are not considered (e.g. underfrequency protection relays), assuming that network operator is solely responsible for returning the overstressed system into the normal operating region. In order to formulate methodologies that will provide more realistic results, the future work by the authors will include both automatic emergency control/protection systems and system dynamics into the presented analytical framework.

#### ACKNOWLEDGMENT

The authors would like to acknowledge the support by the Principal Career Development and Global Research scholarship from the University of Edinburgh, Scotland, UK.

#### REFERENCES

[1] L. Grigsby, "Power system stability and control", Vol. 5, CRC Press, 2012.  
 [2] O. Alsac, and B. Stott, "Optimal load flow with steady-state security", *IEEE Trans. on Power Apparatus and Systems*, vol. 3, pp 745-751, May, 1974.  
 [3] J. A. Momoh et al., "Challenges to optimal power flow", *IEEE Trans. on Power Syst.*, vol. 12, no. 1, pp. 444-455, Feb. 1997.  
 [4] B. Stott, O. Alsac, "Optimal power flow—basic requirements for real-life problems and their solutions", *SEPOPE XII Symposium*, Brazil, 2012.  
 [5] J. Gunda, S. Djokic, R. Langella and A. Testa, "Comparison of conventional and metaheuristic methods for security-constrained OPF analysis," *AEIT International Annual Conference (AEIT)*, Naples, 2015, pp. 1-6.

[6] J. Gunda, G. Harrison, S.Z. Djokic, "Analysis of Infeasible Cases in Optimal Power Flow Problem", *IFAC-PapersOnLine*, vol. 49, Issue 27, pp. 23-28, 2016.  
 [7] J. Gunda and S. Djokic, "Coordinated Control of Generation and Demand for Improved Management of Security Constraints," *IEEE PES ISGT Conf.*, Ljubljana, Slovenia, Oct. 10-12, 2016.  
 [8] D. Fang, J. Gunda, and S. Djokic, "Security—and Time—Constrained OPF Applications", *IEEE PES PowerTech Conf.*, Manchester, 2017.  
 [9] Power Systems Engineering Research Centre (PSERC), "MATPOWER: A MATLAB Power System Simulation Package" [Online] <http://www.pserc.cornell.edu/matpower/>  
 [10] Siemens PTI. (2011). Power Technologies Inc. *PSS/E*, 33.  
 [11] M. A. Abido, "Optimal power flow using particle swarm optimization", *Int. J. of El. Power & Energy Syst.*, vol 24, no. 7, pp. 563-571, 2002.  
 [12] *IEEE standard for calculating the current-temperature relationship of bare overhead conductors*, IEEE Std. 738, 2006.  
 [13] Southwire, "ASCR - Aluminium Steel Reinforced. Bare Conductor," Manufacturer Specification data. [Online] Available at: <http://www.southwire.com/ProductCatalog/proddetail.jsp?htmlpreview=true&token=16&desc=ACSR>  
 [14] H. Wan, J. D. McCalley and V. Vittal, "Increasing thermal rating by risk analysis," *IEEE Trans. on Power Syst.*, vol. 14, no. 3, pp. 815-828, Aug. 1999.  
 [15] S. Foss, S. Lin and R. Fernandes, "Dynamic Thermal Line Ratings Part I Dynamic Ampacity Rating Algorithm", *IEEE Trans. on Power Apparatus and Syst.*, vol. PAS-102, no. 6, pp. 1858-1864, June 1983.  
 [16] IEEE 14-Bus Test Network. [Online] Available at: [http://www2.ee.washington.edu/research/pstca/pf14/pg\\_tca14bus.htm](http://www2.ee.washington.edu/research/pstca/pf14/pg_tca14bus.htm)  
 [17] Y. C. Chen, A. D.-García and P. W. Sauer, "Measurement-Based Estimation of Linear Sensitivity Distribution Factors and Applications," *IEEE Trans. on Power Syst.*, vol. 29, no. 3, pp. 1372-1382, May 2014.  
 [18] Balancing services, National Grid, UK (Dec 2016). [Online]. Available: <http://www2.nationalgrid.com/uk/services/balancing-services/>